ISSN 0021-3640, JETP Letters, 2016, Vol. 104, No. 10, pp. 702–708. © Pleiades Publishing, Inc., 2016.
Original Russian Text © S.V. Filatov, S.A. Aliev, A.A. Levchenko, D.A. Khramov, 2016, published in Pis'ma v Zhurnal Eksperimental'noi i Teoreticheskoi Fiziki, 2016, Vol. 104, No. 10, pp. 714–720.

PLASMA, HYDRO- AND GAS DYNAMICS

Generation of Vortices by Gravity Waves on a Water Surface

S. V. Filatov[a, b, *], S. A. Aliev[a, c], A. A. Levchenko[a–c], and D. A. Khramov[b, c]

[a] *Institute of Solid State Physics, Russian Academy of Sciences, Chernogolovka, Moscow region, 142432 Russia*
[b] *Institute for Theoretical Physics, Russian Academy of Sciences, Chernogolovka, Moscow region, 142432 Russia*
[c] *Astrakhan State University, Astrakhan, 414056 Russia*
** e-mail: fillsv@issp.ac.ru*

Received September 12, 2016; in final form, October 7, 2016

The generation of a vortex motion on a water surface by gravity waves at frequencies of 3 and 4 Hz and wavelengths of 17 and 9.7 cm, respectively, has been studied experimentally. It has been shown that the results can be described by a model of the formation of a vorticity by nonlinear waves. It has been shown for the first time that the vorticity amplitude on a water surface depends on the phase difference between the waves propagating at an angle of 90° with respect to each other and with a period of 360°. A quadratic dependence of the surface vorticity amplitude on the angular amplitude of the waves has been observed. Transfer of the energy of the vortex motion from the pumping region to a larger scale has been discovered.

DOI: 10.1134/S0021364016220082

INTRODUCTION

The spectrum of waves on the surface of an infinitely deep liquid is given by the expression

$$\omega^2 = gk^2 + \frac{\sigma}{\rho}k^3, \quad (1)$$

where ω is the circular frequency of the wave, g is the acceleration of gravity, k is the wave vector, σ is the surface tension, and ρ is the density of the liquid. Waves on a water surface with the wavelength longer or shorter than $\lambda_0 = 2\pi(\sigma\rho/g)^{1/2} = 1.7$ cm are commonly referred to as gravity and capillary waves, respectively. The boundary frequency is $\omega/2\pi = 13$ Hz. The leading term in Eq. (1) at frequencies of 3 and 4 Hz is the first gravity term. It is greater than the capillary term by a factor of 60 and 30 at frequencies of 3 and 4 Hz, respectively, which justifies the classification of surface waves in this frequency region as gravity waves.

The generation of vortices on a water surface by Faraday waves was first observed in [1, 2]. In our previous work [3], we observed the formation of a vortex flow by surface waves in a vessel with a liquid making harmonic oscillations in the vertical direction at pumping amplitudes below the parametric instability threshold. It was found that the generation of vortices is caused by the interaction of nonlinear waves propagating at an angle with respect to one another. The theoretical model describing the formation of vortices by waves was proposed in [4], where it was shown that the generation of a vorticity on the surface of a liquid is due to the nonlinear interaction of surface waves propagating at an angle with respect to each other.

The vorticity Ω on the surface of a liquid is defined as

$$\Omega = \frac{\partial V_x}{\partial y} - \frac{\partial V_y}{\partial x}, \quad (2)$$

where V_x and V_y are the components of the velocity of the liquid.

When standing waves with the frequency ω are excited on the surface of a liquid in two perpendicular directions, the vorticity Ω depends on the wave amplitudes H_1 and H_2, the wave vector k, and the phase difference ψ between the waves and is described by the expression

$$\Omega = -(2+\sqrt{2})\sin(\psi)H_1H_2\omega k^2\sin(kx)\sin(ky). \quad (3)$$

The vorticity amplitude Ω_0 in the case of standing waves is

$$\Omega = \Omega_0\sin(kx)\sin(ky). \quad (4)$$

In the case of waves traveling along the surface, the vorticity is independent of the phase difference ψ and is given by the expression

$$\Omega = -(2+\sqrt{2})\sin(\psi)H_1H_2\omega k^2\sin(kx-ky). \quad (5)$$

The experimental results on the generation of vortices by standing and traveling capillary waves at frequencies of about 40 Hz in a 5.0×4.9-cm rectangular cell were presented in [3, 4]. The wavelength at a frequency of 40 Hz is approximately 0.7 cm. As was found, the amplitude dependences of the vorticity for

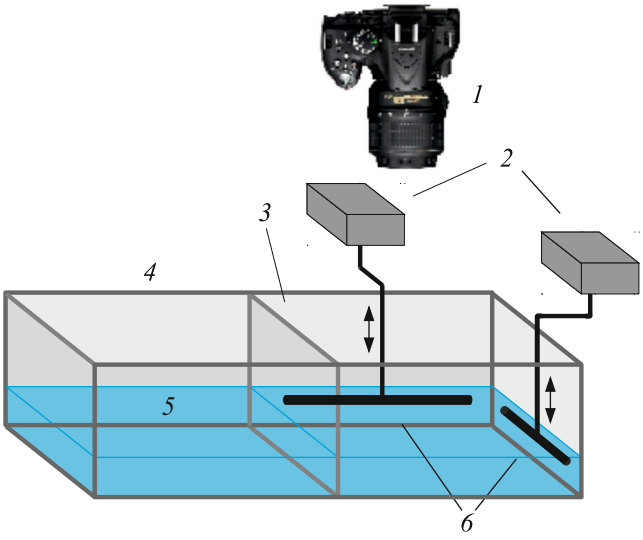

Fig. 1. (Color online) Scheme of the setup with the (*1*) camera, (*2*) plunger drives, (*3*) separating wall, (*4*) bath, (*5*) water, and (*6*) plungers.

traveling and standing capillary waves are described qualitatively well by Eqs. (3) and (5), but there is a disagreement by a factor of 2–5 in the absolute value of the vorticity Ω.

According to [4], dependences (3) and (5) are universal and should hold for both capillary and gravity waves. Thus, this work was aimed at studying the amplitude and phase dependences of the vorticity modulus under the excitation of a surface by gravity waves and investigating the energy distribution over the wave vectors. We present the experimental results of studying the generation of vortices on a water surface by gravity waves at frequencies of 3 and 4 Hz and wavelengths of excited resonance modes of 17 and 9.7 cm, respectively.

EXPERIMENT

Figure 1 shows the scheme of the experimental setup for studying the vortex and wave motions on a water surface in the wavelength range from 0.25 to 20 cm. The bath was made of Plexiglas with a thickness of 10 mm. The length, width, and height of the bath were 140, 70, and 40 cm, respectively. The edges and upper rims of the bath were reinforced by metallic angle profiles to avoid the development of low-frequency oscillations during the operation of wave generators. The bath was divided into two halves by a removable wall. In these experiments, half of the 70×70-cm bath was used. The bath was covered from the top by a transparent glass to prevent air dust particles from coming to the water surface.

The bath was mounted on a Standa vibration-isolating table with a pneumatic support. As a rule, the bath was filled with about 70 L of purified distilled water. The depth of water in the bath was about 10 cm.

The wave generators each consisting of a drive *1* and a plunger *2* were fixed to a frame and mounted to the Standa table. The waves on the water surface were excited by the plunger, a stainless still tube with a diameter of 10 mm half-immersed into water and making vertical oscillations. The length of the tube was 68 cm; the distance from the tube to the bath wall was 1 cm. The drives of the wave generators were Pioneer TS-W254R subwoofers with a nominal power of 250 W. The sinusoidal signals were produced by an Agilent 33522B double-channel generator, amplified, and fed to the subwoofers. The phase difference ψ between the signals was controlled in the experiment. The amplitude of the waves propagating from the plungers was measured in the center of the bath by a laser beam reflected from the surface.

To visualize the motion of the liquid, a white polyamide powder with an average particle diameter of about 30 μm was poured on the water surface. The density of particles was a bit lower than the density of water, so that they were immersed. Therefore, we assumed that the particles were completely dragged by the water flow. The granules on the surface stuck together into coarser formations with a size on the order of 1 mm. We managed to break them into smaller clusters by intense excitation of the surface. The particles on the surface were illuminated by light-emitting diodes situated along the perimeter of the bath. Video of the oscillating surface was recorded for 60 s by a Canon EOS 70D camera at a rate of 24 fps. Such a rate allows choosing the frames of the oscillating surface at the same phase of the wave. For example, at a driving force frequency of 3 Hz, a time interval of 10 s includes 30 frames in series where the exciting surface waves are in the same phase. Such a selection of frames allows excluding from further processing the oscillating component of the displacement of a probe particle floating on the surface. To identify tracks of particles on the surface, frames are summed.

Processing of the original frames by PIVLab software [6] allows computing the particle velocities V_x and V_y and then calculating the surface vorticity with the use of Eq. (2). The energy distribution over the wave numbers can be calculated by averaging the energy over the spatial ring by the formula

$$E(k) = \frac{1}{2S\Delta k}\int \frac{d^2q}{(2\pi)^2}\left\lfloor |V_k|^2 \right\rfloor, \qquad (6)$$

where the integration is performed over the ring from k to $k + \Delta k$. The resulting value is normalized to the surface area S of the liquid. Here, V_k is the Fourier component of the velocity of the liquid. The brackets $\lfloor\ \rfloor$ denote averaging over the frames taken at different times.

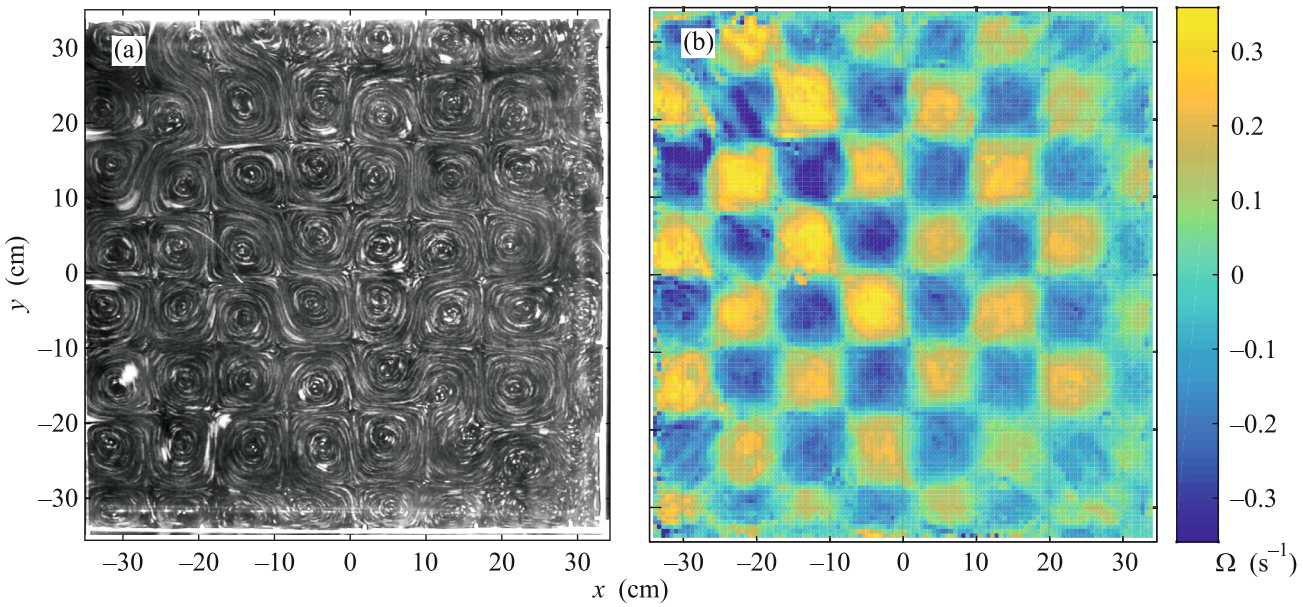

Fig. 2. (Color online) (a) Tracks of polyamide particles on the water surface under pumping by two plungers at a frequency of 3 Hz and the angular amplitude $\mu = 0.035$ rad of the wave in the center of the bath. The plungers are situated at the bottom and on the right-hand side of the figure. (b) Distribution of the vorticity on the water surface under pumping by two plungers at a frequency of 3 Hz and the phase difference $\psi = 90°$.

The group velocity of the wave at a frequency of 3 Hz is 25 cm/s. Thus, the traveling wave passes double the distance between the plunger and the wall, i.e., 136 cm, in 5.5 s from switching on the pumping to the emergence of a standing wave on the water surface. In the results presented below, we calculated the vorticity and energy distributions from the data collected for 5 s starting from 15 s after switching on the pumping to be sure that the amplitudes of standing waves and the vorticity reached the steady state. According to our measurements, the vorticity modulus starts to slightly decrease at times greater than 30 s after switching on the pumping.

RESULTS

Figure 2a shows the tracks of polyamide particles under pumping of the water surface at a frequency of 3 Hz. A lattice of vertical and horizontal rows of vertices similar to that reported in [1] is well seen on the water surface at moderate pumping amplitudes. The average velocity of polyamide particles is 0.02 cm/s. Figure 2a presents the picture averaged over 10 s starting from 15 s after switching on the pumping.

Figure 2b shows the distribution of the vorticity found by processing the sequential images by PIVLab software. As is clearly seen, the lattice formed in the bath consists of small vortices of close sizes and opposite vorticities. The lattice periods in the X and Y directions are 17 cm and coincide with the wavelength of the standing wave that appeared under the 3-Hz pumping. The total vorticity on the bath surface is zero.

The vorticity amplitude of each vortex on the water surface increases with the pumping level. Figure 3a shows the square root of the average vorticity amplitude $\sqrt{\Omega_0}$ of the vortices on the water surface as a function of the angular amplitude of the standing wave measured in the center of the bath. The phase difference ψ between the signals supplied to the plungers is 90°. It is clearly seen that the vorticity amplitude increases quadratically with the wave amplitude, in accordance with Eq. (3).

Figure 3b shows the vorticity amplitude on the water surface as a function of the phase difference ψ between the harmonic signals at a frequency of 3 Hz supplied to the plungers. As is seen, the experimental points fit well the dependence proportional to $\sin\psi$ within the angle range from 0° to 180°. The vorticity amplitude is conserved under a change in the phase difference ψ from 90° to –90°, but the directions of the vorticity in the lattice change to the opposite ones. Thus, the period of the function $\Omega(\psi)$ is 360°.

The picture of tracks becomes more complicated at a high pumping level: a vortex lattice is formed right after switching on the pumping and then, after a minute or so, structures larger than the pumping wavelength develop on the surface. The trajectories (tracks) of particles evolve slowly with time; the vortices "breathe."

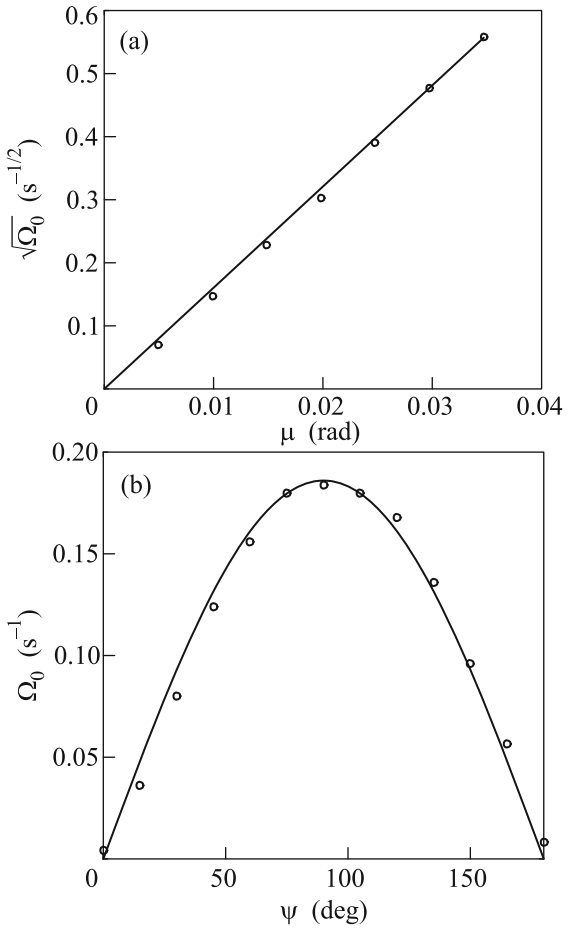

Fig. 3. (a) Square root $\sqrt{\Omega_0}$ of the vorticity amplitude on the water surface versus the angular amplitude μ of the waves under pumping by two plungers at a frequency of 3 Hz and the phase difference $\psi = 90°$. (b) Vorticity amplitude Ω_0 versus the phase difference between the sinusoidal signals supplied to the wave generators according to (points) the experiment and (solid curve) the formula $\Omega_0 = 0.183\sin\psi$.

Figure 4a shows the tracks of polyamide particles on the water surface under pumping at a frequency of 4 Hz found by averaging over 15 s starting from 3 min after switching on the pumping. The wave amplitude measured at a distance of 3 cm from the plungers is (1.0 ± 0.2) mm. In Fig. 4a, one can clearly see two formed vortices with the characteristic sizes close to 70 cm (the length of the bath sidewall), as well as smaller vortices. The phase difference in these measurements was $\psi = 120°$.

Figure 4b shows the vortex structure generated by standing waves at a frequency of 4 Hz. Each side of the bath matches seven wavelengths; i.e., the wavelength at the pumping frequency is 9.7 cm. One can clearly see a vortex lattice slightly distorted by two large vortices in the lower and upper parts of the picture. The total vorticity is zero. Figure 5 presents the absolute value $|\Omega|$ of the total vorticity on the water surface excited by two plungers at a frequency of 4 Hz as a function of the phase difference ψ between the oscillations of the plungers.

The initial phase difference between the oscillations of the plungers is $-30°$. The maximum and minimum of the vorticity modulus occur at $\psi = 120°$ and 30°, respectively. In addition, the dependence $|\Omega(\psi)|$ obviously has a constant component of approximately 0.08 s^{-1}.

As is seen in Fig. 4, under the intense and long pumping, large vortices appear on the water surface in addition to the lattice of small vortices. This implies that the vorticity Ω and the energy E propagate in the k space from the pumping region with $\lambda = 9.7$ cm to larger scales.

The calculated distributions $E(k)$ for the vortex structures shown in Figs. 2 and 4 are presented in Fig. 6 (curves *1* and *2*). The dependence $E(k)$ is clearly nonmonotonic. In the case of the excitation of the surface by waves at a frequency of 4 Hz, there is a pronounced peak at the wave vector $k = 0.50$ cm^{-1}, coinciding with the wave vector of pumping. In addition, there is a peak at the wave vector $k = 1.12$ cm^{-1}. This peak can be presumably associated with the formation of the vorticity owing to the interaction between the wave generated at the pumping frequency and the perpendicular wave with a wave vector of 1.06 cm^{-1} (the respective wavelength is one-third of the pumping wavelength). The energy transfer to larger scales does not occur.

However, in the case of pumping at a frequency of 4 Hz (Fig. 6, curve *2*) and the formation of surface vortex structures larger than the pumping scale, the energy $E(k)$ is distributed over the wave vectors ranging from the pumping region $k \approx 0.85$ cm^{-1} to large scales with $k \approx 0.09$ cm^{-1}.

The first peak at the wave vector $k = 0.85$ cm^{-1} is situated within the pumping region. This energy is concentrated in small vortices, which form a lattice. Clearly, $E(k)$ increases with a decrease in k. The maximum of the distribution $E(k)$ falls to the wave vector close to 0.09 cm^{-1}, which corresponds to the size of large vortices formed in the bath. The additional curve *3* in Fig. 6 shows the distribution $E(k)$ under pumping by waves with a shorter wavelength (frequency of 6 Hz, wavelength of 4.9 cm). This distribution also exhibits two extrema corresponding to the pumping scale, $k = 1.8$ cm^{-1}, and the energy maximum, $k = 0.1$ cm^{-1}. Comparison of distributions *2* and *3* leads to a conclusion that the size of a large vortex is independent of the pumping wavelength, being determined by the dimensions of the bath. The $E(k)$ values in the region of the wave vectors $k > 2$ cm^{-1} are more than an order of magnitude lower than the amplitudes of the main peaks. That is, the direct cascade is hardly formed: the

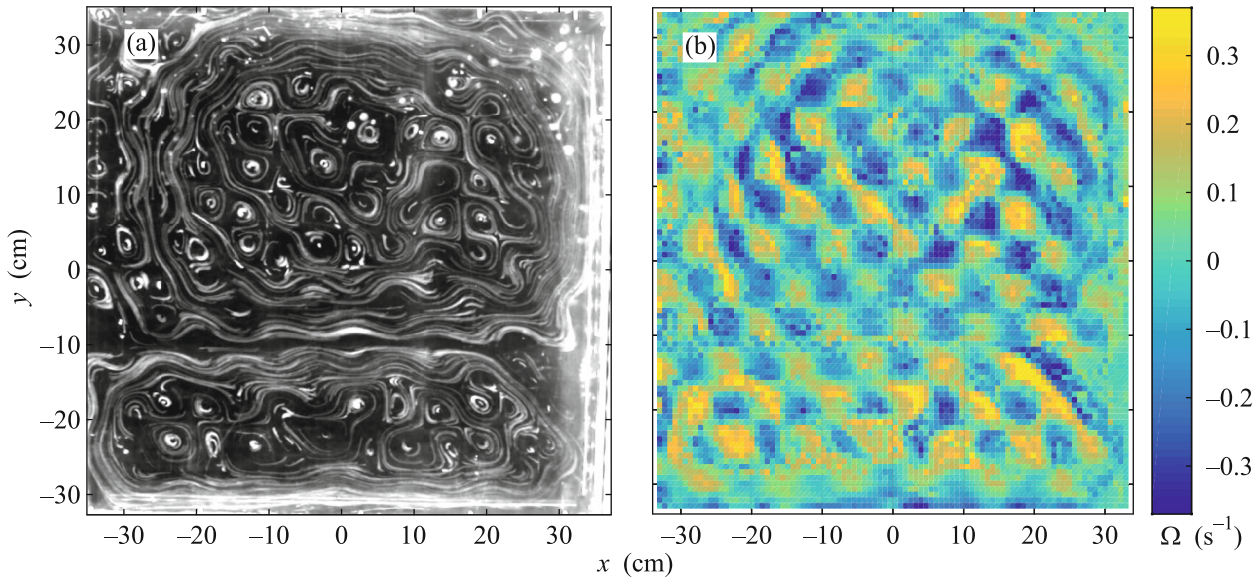

Fig. 4. (Color online) (a) Tracks of polyamide particles on the water surface under pumping by two plungers at a frequency of 4 Hz. The amplitude of the waves at a distance of 3 cm from the plungers is $H = (1.0 \pm 0.2)$ mm. The plungers are situated at the bottom and on the right-hand side of the figure. (b) Distribution of the vorticity on the water surface. The phase difference is $\psi = 120°$.

energy is spent entirely for maintaining large vortices, where it is dissipated owing to viscous losses.

DISCUSSION

As in [3, 4], we observe in this work a vortex lattice with a lattice constant equal to the pumping wavelength. This indicates the validity of the model of the generation of vortices by nonlinear waves and justifies the use of Eqs. (3) and (5) to describe the vorticity on the surface of a liquid in a wide range of wavelengths from 0.5 to 17 cm. It is worth mentioning that the vortex lattice under pumping at a frequency of 3 Hz (Fig. 2) is as perfect as under pumping by capillary waves [4], in which case the measurements were carried out in a special box with a pure atmosphere. In the case of gravity waves, a thin incompressible film is formed on the water surface in about 1 h if the bath is not covered from the top, which results in a considerably higher damping of waves [5], as indicated by the distribution of the vorticity.

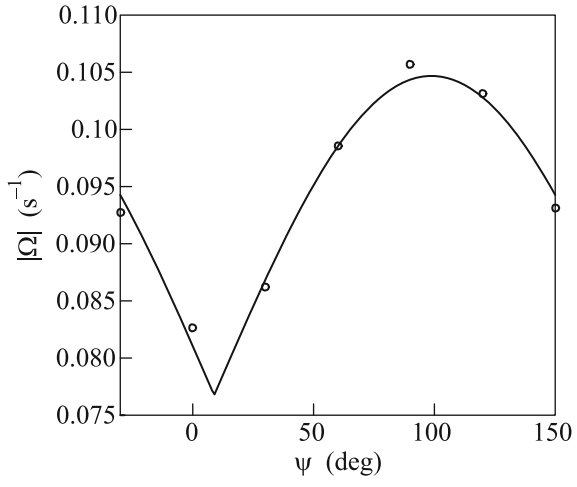

Fig. 5. Vorticity modulus on the water surface versus the phase difference ψ between the oscillations of the plungers at a frequency of 4 Hz. The amplitude of the wave at a distance of 3 cm from the plungers is $H = (1.0 \pm 0.2)$ mm.

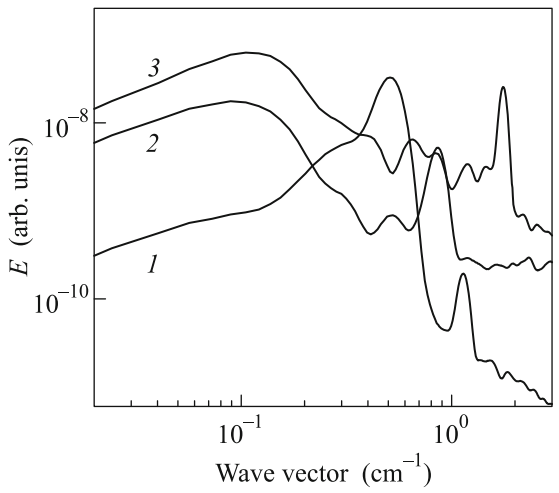

Fig. 6. Energy distribution $E(k)$ over the wave vectors under pumping by two plungers at a frequency of (*1*) 3, (*2*) 4, and (*3*) 6 Hz.

Damping of waves is insignificant in Figs. 3b and 4b, which show the vortex lattices. The amplitude of the wave reflected from the bath wall is nearly the same as the amplitude of the counterpropagating wave traveling from the plunger. According to Eqs. (3) and (5), a difference between these amplitudes should not affect the quadratic dependence of the vorticity on the wave amplitude.

The phase dependence of the vorticity amplitude under the excitation of waves by two plungers at a frequency of 3 Hz fits very well a periodic function proportional to $\sin\psi$. The period of the function $\Omega(\psi)$ is 360°, in agreement with Eq. (3).

A somewhat more complicated situation takes place in the experiments on studying the dependence of the vorticity modulus on the phase difference ψ between two perpendicular excitation waves at a frequency of 4 Hz. As was mentioned above, there are both vortices forming a lattice on the water surface and larger vortices that appear owing to the nonlinear interaction of the vortices and waves. This is clearly seen in Fig. 4a, in which there are both a lattice of individual vortices and large vortices on the surface. Accordingly, the phase dependence of the vorticity cannot be described by Eq. (3) and should include a term reflecting the presence of larger vortices. As is seen, pumping of vortices does not disappear even at $\psi = 0°$; i.e., the presence of large-scale vortex flows complicates the generation of vortices by nonlinear surface waves described by simple relations (3) or (5). The quantity $|\Omega|$ oscillates about some pedestal. It cannot be concluded from the results of the present experiments whether the height of this pedestal changes with an increase in the phase difference; hence, we assume it to be constant in the first approximation.

The found experimental result qualitatively does not contradict the model presented in [4]. As is seen in Fig. 5, the dependence of $|\Omega|$ on the phase difference ψ has a periodic character with two extrema. The period is 180°. Thus, the dependence of the vorticity modulus $|\Omega|$ on the phase difference can be described by the formula

$$|\Omega| = A|\sin(\psi + \psi_0)| + \Omega_0, \qquad (7)$$

where ψ_0 is the initial phase shift and Ω_0 is a constant. Fitting of the experimental data to Eq. (7) yields $\psi_0 = -9°$, $\Omega_0 = 0.077$ s^{-1}, and $A = 0.028$ s^{-1}. It is worth mentioning that the constant term is determined by the structure of large vortices that appear on the surface and varies from one experiment to another under the same initial conditions.

It should be mentioned that the absolute values of the vorticity modulus obtained in the experiments on measuring the dependence of the vorticity amplitude on the wave amplitude and phase difference are approximately four times greater than the theoretical value calculated by Eq. (3). A similar discrepancy was observed in [4] in the case of capillary waves.

It should also be mentioned that, under pumping at low frequencies corresponding to gravity waves, the formation of a vortex structure with a characteristic size greater than the pumping scale was always observed sometime after the pumping was switched on. One or a few large vortices can occupy almost the whole surface of the bath except small regions, where "smearing" vortices, which assure zero total vorticity, are situated. It is also worth mentioning that large vortices appeared in the experiments with capillary waves only above the parametric instability threshold [2].

As follows from the dependences shown in Fig. 6 (curves *2* and *3*), the energy of the vortex motion is transferred from the pumping region to larger scales. Obviously, the energy of surface waves is first transferred to a system of vortices arranged in a lattice. Next, owing to the nonlinear interaction, the energy is distributed to larger scales. Clearly, the energy is mainly transferred to coarse vortices and does not go toward smaller scales: a direct cascade toward high k values (small scales) hardly occurs.

The inverse cascade was previously observed in the experiments on the generation of surface Faraday waves [7]. It turned out that the experimental distribution of energy over the wave vectors can be described well by the dependence $E(k) \sim k^{-5/3}$. This dependence for the inverse energy cascade was predicted theoretically by Kraichnan [8] for thin two-dimensional liquid layers. In the case of the direct cascade, $E(k) \sim k^{-3}$ [8]. In our experiments, the pumping and dissipation regions are not sufficiently far apart in the k space for the formation of a developed cascade described by a power function of k.

It should be emphasized that we deal with the three-dimensional case in our experiments, since the bath depth is greater than the penetration depth of the waves at all pumping frequencies we used. However, the energy transfer from the pumping region to larger scales inherent in the two-dimensional case certainly takes place.

The discrepancy between the experimental absolute value of the vorticity and the theoretical estimate and the formation of the inverse cascade inherent in two-dimensional systems in our three-dimensional experiments require further experimental and theoretical investigations.

CONCLUSIONS

In this work, it has been experimentally demonstrated for the first time that the vorticity formed on the water surface by weakly nonlinear gravity waves depends on the phase difference between the waves and is described well by the expression derived in [4]. The vorticity amplitude on the surface depends qua-

dratically on the wave amplitude. Thus, the model of the generation of a vortex motion by nonlinear waves is applicable to the description of the vorticity on the surface of a liquid for both the waves in the capillary range with a wavelength of about 0.5 cm and gravity waves with wavelengths on the order of 10 cm. In our experiments, we have observed the energy transfer from weakly nonlinear wave motion to the system of vorticities forming a lattice with further redistribution to larger scales.

We are grateful to V.V. Lebedev, I.V. Kolokolov, S.S. Vergeles, L.P. Mezhov-Deglin, and E.I. Kats for fruitful discussions. This work was supported by the Russian Foundation for Basic Research, project no. 14-22-00259.

REFERENCES

1. A. von Kameke, F. Huhn, G. Fernández-Garcia, A. P. Muñuzuri, and V. Pérez-Muñuzuri, Phys. Rev. Lett. **107**, 074502 (2011).
2. N. Francois, H. Xia, H. Punzmann, and M. Shats, Pys. Rev. Lett. **110**, 194501 (2013).
3. S. V. Filatov, M. Yu. Brazhnikov, and A. A. Levchenko, JETP Lett. **102**, 432 (2015).
4. S. V. Filatov, V. M. Parfenyev, S. S. Vergeles, M. Yu. Brazhnikov, A. A. Levchenko, and V. V. Lebedev, Phys. Rev. Lett. **116**, 054501 (2016).
5. L. D. Landau and E. M. Lifshitz, *Course of Theoretical Physics,* Vol. 6: *Fluid Mechanics* (Nauka, Moscow, 1986; Pergamon, New York, 1987).
6. W. Thielicke and E. J. Stamhuis, J. Open Res. Software **2**, 30 (2014).
7. N. Francois, H. Xia, H. Punzmann, S. Ramsden, and M. Shats, Phys. Rev. X **4**, 021021 (2014).
8. R. H. Kraichnan, Phys. Fluids **10**, 1417 (1967).

Translated by A. Safonov